BEAM LOSS SIMULATION STUDIES FOR ALS TOP-OFF OPERATION*

H. Nishimura, D. Robin, C. Steier and R. Donahue, LBNL, Berkeley, CA 94720, U.S.A

Abstract

ALS[1] has been proposing the Top-off injection[2] of the electron beam. As a part of its radiation safety study, we carried out two kinds of tracking studies: (1) to confirm that the injected beam cannot go into users' photon beam lines, and (2) to control the location of the beam dump when the storage ring RF is tripped. (1) is done by tracking electrons from a photon beam line to the injection sector inversely by including the magnetic field profiles, varying the field strength with geometric aperture limits to conclude that it is impossible. (2) is done by tracking an electron with radiation in 6-dim space for different combinations of vertical scrapers for the realistic lattice with errors.

INVERSE PARTICLE TRACKING

Principle

When the top-off injection becomes reality, we must make sure that the injected electron beam does not go into the users' photon beam ports. We study this scenario for the beam line BL2.1 that is the closest to the injection point of the storage ring. In Fig.1, the BTS is the beam transport line from the booster ring to the storage ring. The injection point is in straight section 1 which is followed by the arc section 1, straight section 2. Then the beam goes through the bending magnet 2.1 that is at the beginning of arc sector 2. The photon beam line 2.1 is for the synchrotron radiation from this bend and the first user's port that the injected electron beam sees. We must confirm there is no possibility of the electron beam going into this port.

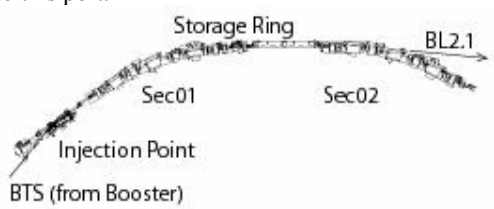

Figure 1: Sector 01 and 02 of the ALS storage ring.

Requirements

Backwards tracking from BL2.1 towards the injector - same approach was taken following APS[3] and ESRF[4]. It was done in the horizontal plane with the following conditions:

(1) Magnet settings: Assume stored beam and check all the possible situations of top-off injection by varying the magnets.

*Work supported by the U.S. Department of Energy under Contract No. DE-AC03-76SF00098

(2) Initial conditions: Using apertures in the beam line front end, determine the available phase space of the beam line relative to the storage ring.
(3) Magnetic Field Profiles:
(4) Apertures: The aperture must be checked along the path.

Method of Simulation

We used a C++ class library[5] by adding special routines to track through the field with transverse profiles.

The tracking was done in the horizontal plane.

(1) Table 1 shows the magnets for parameter scanning. Their scanning ranges and step sizes are also listed.

Table 1 Magnet Setting Scan Parameters

Magnet	# of Magnets	Scan Range	Step Size
Quad	9	-20% ~ 20%	2 %
Sext	6	0 ~ 200%	20%
Steering	11	-1 ~ 1 mrad	0.1 mrad

There are 4 bending magnets in the area but not listed here. Instead of scanning bending magnets, we vary the energy from 0 to 200% by every 1%.

We change magnets one at a time, and scan the energy for each one of them. The total number of cases is ~ 98×10^3.

(2) Using the aperture geometry in the beam line front end, determine the available phase space of the beam line relative to the storage ring. The result is shown in Fig. 2 which determines the range of initial conditions of the backward tracking. The reference is at X_0=334.87 mm and Px_0 = -240.517 mrad.

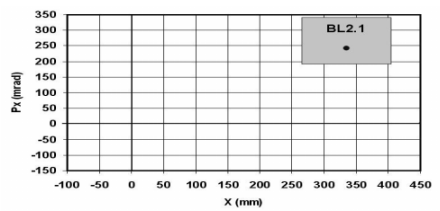

Figure 2: Initial conditions of the backward tracking.

The range of initial condition, the grey rectangle in Fig. 2, is summarised in Table 2.

Table 2 Initial Condition Scan Parameters

	Scan Range	Step Size
dX_0	-70~ 70 mm	1 mm
dPx_0	-50 ~ 100 mrad	1 mrad

Therefore, we scan for $141\times151= 21\times10^3$ initial conditions for each magnet/energy setting, which makes the total of 2.1×10^9 cases to track.

(3) Use the transverse field profile of the magnets, Fig. 3. Quadrupole and sextupole fields are to be scaled to their settings. Steering magnets are assumed to be linear.

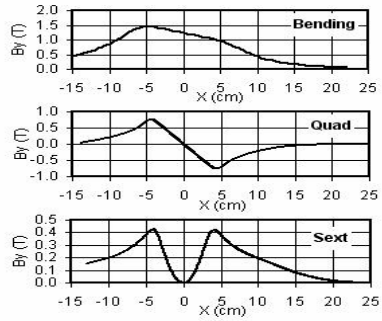

Figure 3: Horizontal magnetic field profiles [x].

(4) Quad and bending magnets are longitudinally segmented into 100 steps and the aperture is checked at every step. On the other hand, sextupole and steering magnets are modelled as thin kicks.

Result

There are total of ~2.1×10^9 cases. The distance between the real injection point and the initial position of the backward tracking at BL2.1 is 25.2 m. Fig. 4 shows how much a beam can travel from BL2.1 toward the real injection point as a function of its energy. The maximum length is 21.9 m that is at the edge of the defocusing quad (QD) in the straight sector 1. There is no case that can reach the real injection point.

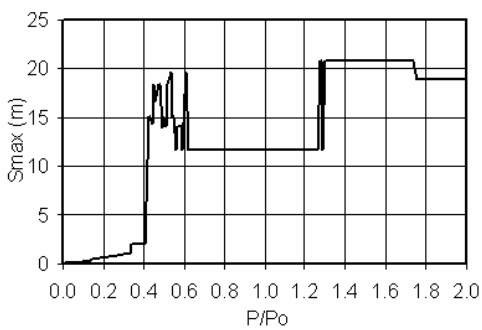

Figure 4: Maximum travelling length (Smax) of beam tracked backwards as a function of energy (P/P_0).

The worst 5 cases are plotted in Fig. 5. The beam is tracked from the right upper point (marked as BL2.1) to left. This figure shows that the straight sector 2 is acting as a filter effectively, which is also shown in FIg.4 where Smax = 11.6 m for P/P_0=0.63 ~ 1.26.

Therefore, this backtracking simulation shows that the injected beam cannot get into BL2.1.

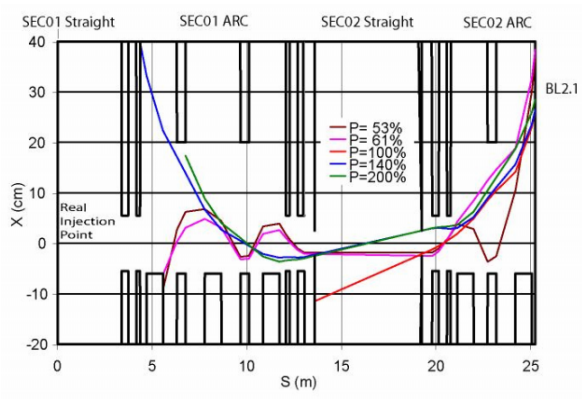

Figure 5: The worst 5 rays of the backwards tracking.

TRACKING WHEN RF TRIPS

Observation

When the RF power suddenly trips by the interlock to dump the circulating beam, higher radiation is often observed at the narrow gap chamber at sector 4 where vertical clearance is ±4 mm, indicating that the beam crashes into the chamber wall. The measurements show that, when the RF trips, the beam circulates about 200 ~ 250 turns without RF.

Energy-dependent tune shift

The beam energy decreases 1% every 70 turns at 1.9 GeV when RF if off by changing the betatron tunes due to energy-dependent tune shift as shown in Fig. 6. The vertical tune hits the integer resonance at about 280 turns in case of an ideal lattice.

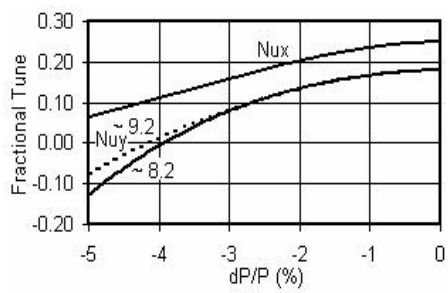

Figure 6: Energy-dependent betatron tune shift.

Interpretation

When the RF trips, the amplitude of the vertical oscillation increases due to the energy-dependent tune shift to hit the narrow vertical aperture given in Table 3. Vertical apertures at sectors 4 and 8 are narrower and are located downstream of wider sections, therefore they are most likely to have a hit by the electron beam. Among these two sectors, sector 4 is equipped with the radiation monitors that are more sensitive than the others, which can explain our observations.

Table 3 Half-Height (mm) of the straight sector chambers

Sec	HH	Sec	HH	Sec	HH
1	7.0	5	4.5	9	8.0
2	9.0	6	7.5	10	8.0
3	9.0	7	5.0	11	4.5
4	4.5	8	5.0	12	8.0

Jackson Holes

The arc chambers have 6 holes (called Jackson holes) of the diameter 2" along the orbit shown in Fig.7. Currently they are closed except for one (sector 4 #1). These holes can be equipped with a vertical scraper/plunger to control the location of the beam dump so that the radiation does not go into the user's beam lines.

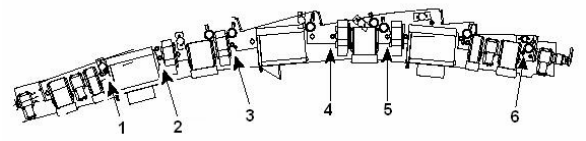

Figure 7: Jackson holes.

Simulation

The model is prepared to track a particle with radiation damping but without RF with realistic random errors to have beam dumps around 200 turns. One simulation uses 100 lattices with different random seeds, and stores the particle trajectories in data files. These trajectories are post-processed for different configurations of the vertical apertures defined by the narrow gap chambers and the Jackson-hole plungers. Fig. 8 shows the simulation program running interactively on the Windows.

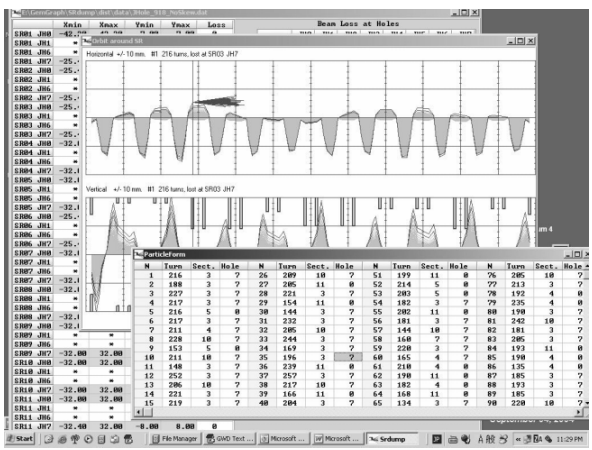

Figure 8: Simulation program on Windows.

Fig. 9 shows one of these results: the beam runs into the beginning of the narrow-gap chamber at sector 4 and creating the radiation to forwards. This is for one particular random seed, and there are total 100 seeds for one set of simulation.

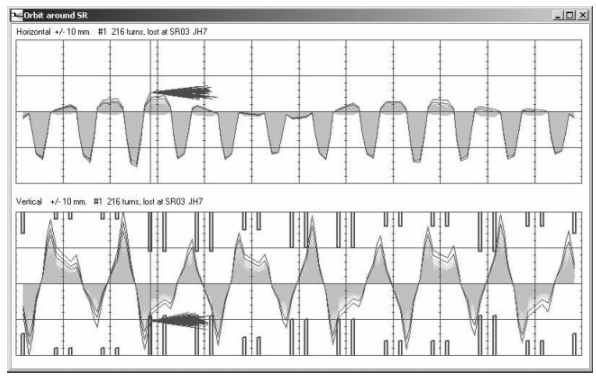

Figure 9: Beam loss at straight section 4.

Here is an example of using the straight section 3 as a location of controlled beam dump. The two Jackson-holes on both sides of it are used to define the gap to limit the vertical aperture. Fig. 10 shows the ratio of beam loss at this sector as a function of the gap.

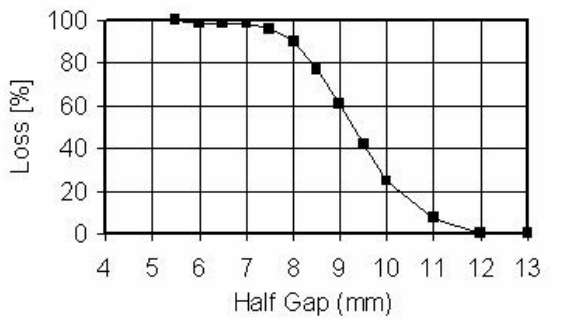

Figure 10: Beam damp at SR02 straight section as a function of its gap.

This program can simulate, as this example shows, the beam loss process when the RF is tripped reasonably. We will be using it to evaluate the effect of plungers we plan to install in the near future.

AKNOWLEDGEMENTS

We thank L. Emery at APS, P. Elleaume, L. Farvacque, P. Colomp at ESRF for useful comments and discussions, Jin-Young Jung for FEM calculations, and B. Fairchild at ALS for his technical assistance.

REFERENCES

[1] LBL PUB-5172 Rev. LBL, 1986.

A. Jackson, PAC'93, Washington D.C, May 1993, P.1432.

[2] D. Robin, et al. EPAC'04, Lucerne, July 2004.

[3] M. Borland, L. Emery, PAC'99, New York, March/April 1999, P2319.

[4] P. Berkvens, P. Colomp, RadSynch04 Workshop, SPRING8, Nov. 2004, Japan.

[5] H. Nishimura, PAC'01, Chicago, July 2001, P.3066.